

Generalised Scale Invariance and Multiplicative Processes in the Atmosphere

D. SCHERTZER¹ and S. LOVEJOY²

Abstract—Many geophysical fields show highly intermittent fractal structures spanning wide ranges of scale. However, few are isotropic: “texture”, stratification, as well as variable (scale dependent) orientation of structures is far more common. To deal with such fractals, we must generalise the idea of scale invariance beyond the familiar self-similar (or even self-affine) notions. Taking the atmosphere as our primary example (however, we also model galaxies), we outline the necessary formalism (generalised scale invariance), and show how it can be used to deal with the strongly intermittent structures which result from multiplicative (cascade type) processes concentrating matter or energy into smaller and smaller scales.

We illustrate these ideas with rain data from blotting paper and radar, showing first how to directly estimate the elliptical dimension characterising the stratification, and second, how to determine universal scale-independent (invariant) codimension functions that characterise the distribution of the intense rain regions.

Key words: Scale invariance (scaling), (multi-) fractal, nonlinear variability, turbulence, geophysics, atmosphere, multiplicative processes.

1. Introduction

Scaling notions are associated with power-law spectra, lack of characteristic scales over wide ranges, and the appearance of fractal dimensions and structures. More precisely, a system may be said to be scaling (or scale invariant) over a range if the small and large scale structures are related by a scale changing operation involving only the scale ratio. The above characteristics are common in many areas of geophysics, and if considered under the general rubric of nonlinear variability, constitute a central, and indeed unifying aspect of geophysical systems.

In recent years, there has been a series of new developments in our understanding of scaling, particularly of scaling fields (measures) including several that were specifically stimulated by geophysical applications. These new ideas involve both the possibility of very general anisotropic types of scaling (necessary, for example to deal with rotation, stratification or “texture”), as well as “multiple scaling”

¹ EERM/CRMD, Météorologie Nationale, 2 Ave. Rapp, Paris 75007, France.

² Physics Dept., McGill University, 3600 University st., Montreal Que., H3A 2T8, Canada.

have different scaling behaviour. These results are important since in geophysics, we are immediately faced with the problem of extremely variable fields rather than with sets of points. While the development of geometrical fractal notions (MANDELBROT, 1982) is often suggestive and has been important, the development of concrete analytical methods has tended to show that geometrical frameworks can often be misleading. Indeed, it seems increasingly clear that fractal notions have been most fruitful when divorced from geometry. Particularly important in this regard has been the abandonment of the dogma of the unicity of fractal dimension in favour of hierarchies of dimensions and singularities defined by nongeometric generators.

Mushrooming interest in geophysical applications of such nonlinear variability has led to two workshops on the theme "Scaling, fractals and Non-linear VARIABILITY in Geophysics I" (NVAG1) in August 1986 at McGill University (LOVEJOY and SCHERTZER, 1988a; SCHERTZER and LOVEJOY, 1988a), and at the former Ecole Polytechnique in Paris France, (NVAG2, June 1988). There has also been a session on fractals in geophysics at the December 1986 AGU meeting (see some of the papers in a forthcoming special issue of *PAGEOPH*).

Below, we outline a number of relevant theoretical developments and give examples of the applications to atmospheric phenomena. Section 2 gives a fairly nonmathematical overview, and sections 3 and 4 outline the geophysical motivation for generalising scale invariance to anisotropic situations, concentrating on the example of the atmosphere. Sections 5 and 6 give a more precise mathematical formulation, including relations to intermittency, singularities and divergence of high order statistical moments. Section 7 discusses some applications to radar rain data and includes two new data analysis techniques, functional box-counting and elliptical dimensional sampling. More detailed developments of the formalism can be found in SCHERTZER and LOVEJOY (1987a,b) and other geophysical applications will be found in the references.

2. Multiple vs Simple Scaling

Perhaps the simplest illustration of scaling and scale invariance is to consider the ("metric" or more exactly "measure") idea of dimension of a set of points. The intuitive (and essentially correct) definition is that the "content" of the set $n(L)$ at scale L is given by:

$$n(L) \propto L^D \quad (1)$$

where D is the dimension (e.g., the length of a line $\propto L$, the area of a plane, $\propto L^2$, the number of *in situ* meteorological measuring stations on the earth in a circle radius $L \propto L^{1.75}$ (LOVEJOY *et al.*, 1986a,b) or the distribution of raindrops on a piece of blotting paper $\propto L^{1.83}$ (see Figures 1a,b and LOVEJOY and SCHERTZER,

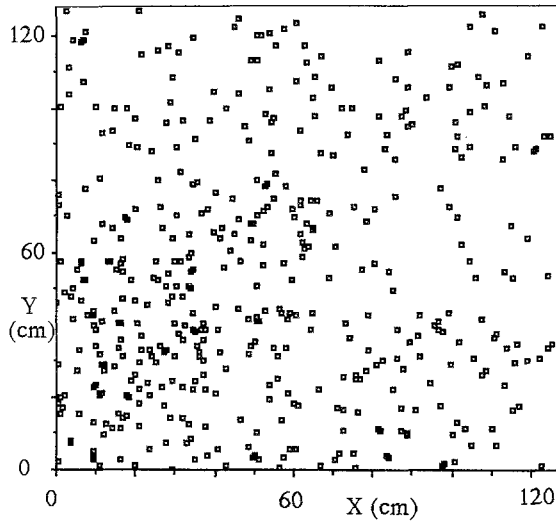


Figure 1a

An empirical illustration of eq. (1) obtained by exposing chemically treated blotting paper (128 × 128 cm in size) for ≈ 1 s in rain. The (452) points represent the drop centres. For a complete analysis, see LOVEJOY and SCHERTZER (1988b).

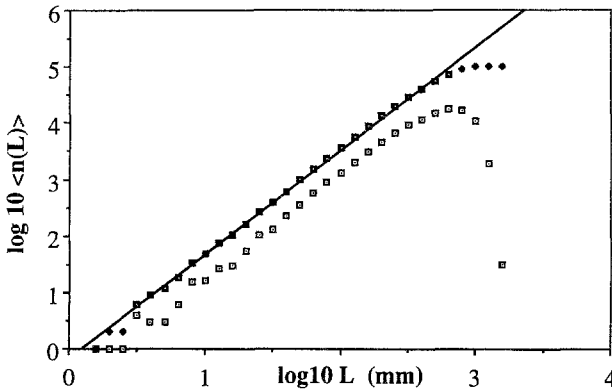


Figure 1b

The function $\langle n(L) \rangle$ measured by determining the average number of drops within a radius L of each drop (this involves $452 \times 451/2 = 101,926$ drop pairs). The $\log L$ - $\log \langle n(L) \rangle$ plot shows D (the slope) ≈ 1.83 . At scales ≤ 2 mm, the finite number of drops leads to deviations, while at scales ≥ 40 cm, the finite size of the paper is important.

1988b). The “volume” (actually the measure of the set) is therefore a simple (power law) function, and the dimension is important precisely because it is scale invariant (independent of L).

In geophysical fluid dynamics the existence of scaling regimes can often be argued directly from the dynamical equations themselves: the only scales associated

with the Navier-Stokes equations are a large-scale involving energy injection, and a small viscous scale where the dissipation occurs. In the atmosphere these scales are roughly the order of thousands of kilometers and several mm respectively, allowing the possibility of a scaling regime spanning over nine orders of magnitude in scale.¹ Furthermore, the notion of scaling regimes in the atmosphere can be traced back to Richardson (the father of numerical weather prediction), who, in the 1920's, suggested a model of atmospheric dynamics involving a self-similar cascade of energy from large to small scales. Since then, scaling ideas have been central to studies of turbulence, a fact that is most notably expressed by the ubiquity of the scaling $k^{-5/3}$ Kolmogorov spectrum of velocity fluctuations in geophysical flows.

The turbulent velocity field (v) affords a convenient example with which to develop the basic scaling ideas. The first scaling of interest, might best be called "simple scaling" since it occurs when only one parameter is sufficient to specify the scaling of all the statistical properties. Assuming statistical invariance and isotropy (including reflectional symmetry), the fluctuation of the velocity depends only on the distance $l (= |l|)$ between the points x and $x + l$:

$$\Delta v(l) = |v(x + l) - v(x)|.$$

In this case, dividing the scale by the scale ratio λ , we reduce the fluctuation by the factor λ^H

$$\Delta v\left(\frac{l}{\lambda}\right) \stackrel{d}{=} \frac{\Delta v(l)}{\lambda^H} \quad (2)$$

(where, $\Delta v(\lambda l) = |v(x + \lambda l) - v(x)|$, and H is the (single) scaling parameter²). The equality (" $\stackrel{d}{=}$ ") is understood in the sense of probability distributions, hence the scaling of the various high order statistical moments follows:

$$\langle \Delta v(l/\lambda)^h \rangle = \lambda^{-\xi(h)} \langle \Delta v(l)^h \rangle \quad (3)$$

with $\xi(h) = hH$, and " $\langle . \rangle$ " means "ensemble average". Since the energy spectrum is the Fourier transform of the covariance, we have a spectrum $k^{-\beta}$ with $\beta = 2H + 1$. If one assumes a scale invariant flux of energy to small scales (the nonlinear terms in the Navier Stokes equations conserve this flux, while breaking up large eddies into smaller and smaller sub-eddies), then dimensional analysis gives $\Delta v(l) \propto \varepsilon^{1/3} l^{1/3}$, hence, $H = 1/3$, $\beta = 5/3$. Note that such a behaviour for the velocity field already leads to velocity fields with interesting properties such as singular

¹ It is worth noting that from the perspective of dynamics, our system is far from equilibrium: it conserves energy fluxes rather than energy.

² It is perhaps worth noting that KEDDEM and CHIU (1987) discuss an even simpler kind of scaling in which the function rather than the differences obey eq. (2) i.e., $v(l/\lambda) \stackrel{d}{=} \lambda^{-H} v(l)$ —hence such processes are not statistically translationally invariant. As pointed out in LOVEJOY and SCHERTZER (1988c) this "very simple scaling" is so simple (and restrictive) that it is unlikely to have geophysical applications.

shears (since $\partial v/\partial x \approx \Delta v/l \approx l^{-2/3}$ which diverges as $l \rightarrow 0$). The problem of such singular behaviour was first discussed by Leray and Von Neumann in the 1930's and 1940's. As we shall see below, that it is indeed central to our current understanding of scaling fields (more precisely, of fractal measures).

In the 1960's, KOLMOGOROV (1962) and OBUHKOV (1962) pointed out that scaling generally involves an infinite number of parameters (e.g. $\xi(h)$ is not generally linear in h , see the discussion in YAGLOM and MONIN, 1975). This is a richer and more interesting behaviour called multiple scaling. The simplest way of expressing this is to consider a scale invariant quantity such as the energy flux ε whose ensemble spatial average is fixed (independent of scale), but, is nonetheless (in a given realisation of the cascade process), highly intermittent. This extreme variability or intermittency can be built up step by step in the cascade process in which large eddies modulate *multiplicatively* the flux to smaller and smaller scales: see schematic diagrams Figures 2a,b and Figures 3a,b,c,d,e. Denote by ε_A , the flux smoothed over a region A (e.g., ε_A is the spatial average over a set A , dimension $D(A)$, divided by the volume of A). In this case, we obtain

$$\langle \varepsilon_{T_\lambda A}^h \rangle = \lambda^{(h-1)C(h)} \langle \varepsilon_A^h \rangle \tag{4}$$

where T_λ is a scale changing operator, that "reduces" by a factor λ . When eq. (4) holds and ε is isotropic, then the required scale change is simply $T_\lambda A = \lambda^{-1}A$ (e.g., a simple reduction by factor λ), and we have a self-similar field (see section 5 for

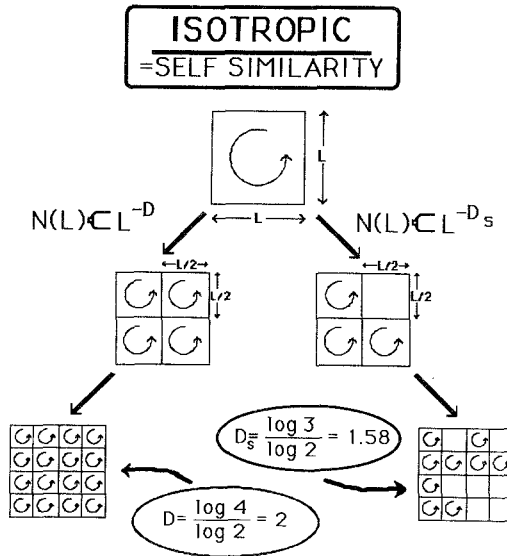


Figure 2a

A schematic diagram showing two steps of an isotropic homogeneous cascade (left), and an inhomogeneous (intermittent) cascade (right).

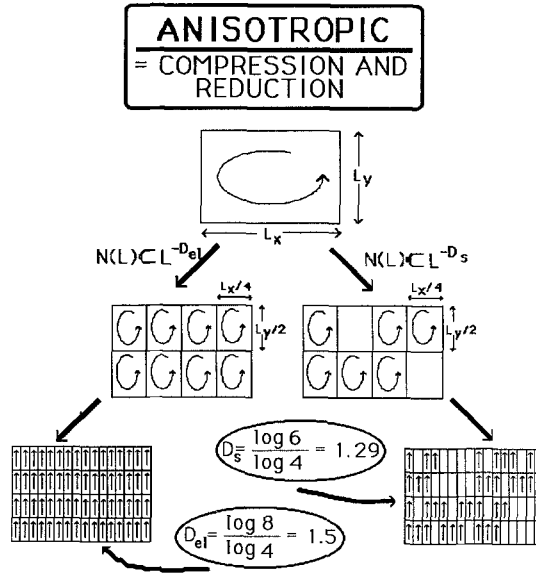


Figure 2b
Same as 2a but for anisotropic case (see section 3).

anisotropy). $C(h)$ is a convex function which for each moment h , can be interpreted as the *codimension* associated with the h^{th} moment. (The codimension is simply the difference between the fractal dimension of a set and the space in which it is embedded—in the meteorological observing network on the earth’s surface $C = 2 - 1.75 = 0.25$.) We have recently shown (SCHERTZER and LOVEJOY, 1987a,b), that in such multiplicative cascades, singularities of all order (γ) are built up progressively as the cascade proceeds to smaller scales, hence as $l \rightarrow 0$, $\varepsilon_l \approx l^{-\gamma}$ with each order of singularity itself, distributed over a set with (different) codimensions $c(\gamma)$ (see section 6 for more details)³. Both families of codimensions ($C(h)$ and $c(\gamma)$) are related by a simple (Legendre) transformation (FRISCH and PARISI, 1985).

These surprising mathematical properties of multiplicative processes are themselves associated with a number of interesting phenomenon (notably the divergence of high order statistical moments, itself related to the existence of statistical “outliers” in the data), and involve fields that are extremely intermittent with statistical properties depending not only on the scale, but also on the dimension (e.g., line, plane or fractal set) over which they are averaged (SCHERTZER and LOVEJOY, 1984, 1985b; LOVEJOY and SCHERTZER, 1988d). This leads to interesting

³ An exception to this hierarchy is the monodimensional “beta model” discussed in NOVIKOV and STEWART (1964), MANDELBROT (1974) and FRISCH *et al.* (1978).

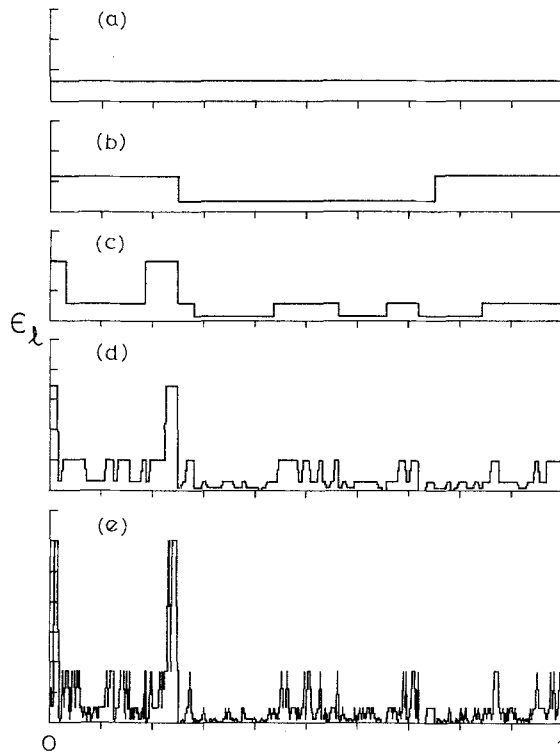


Figure 3

We show a function which starts of homogeneous (constant) over the entire interval shown in a), whose scale of homogeneity is then systematically reduced by successive factors of 4 in b,c,d,e. This is an example of a cascade “ α model” (see SCHERTZER and LOVEJOY, 1985b), which is constructed by multiplying randomly chosen weights over smaller and smaller scales in such a way that on average, the area under the curve (representing the energy flux to smaller scales) is conserved. Because of this constraint, the increasingly high peaks must become more and more sparse. In the limit of the scale of homogeneity going to zero, the function is dominated by singularities distributed over sparse fractal sets.

applications to the problem of measurement and calibration of geophysical data (LOVEJOY *et al.*, 1986a,b; MONTARIOL and GIRAUD, 1986; MARQUET and PIRIOU, 1987; LAVALLÉE *et al.*, 1988; LOVEJOY and SCHERTZER, 1988b; GABRIEL *et al.*, 1988a,b; HUBERT and CARBONNEL, 1988).

3. Scale Invariance as a Geophysical Invariance Principle

We have considered in detail the example of scaling of geophysical fluid systems where scaling ideas have been developed over a considerable period of time. What about other geophysical fields such as the distribution of minerals in the earth’s crust, gravity anomalies, etc.? Even when the dynamical equations are unknown, we can still (following an approach familiar to physicists) argue that at least over

GENERALISED SCALE INVARIANCE

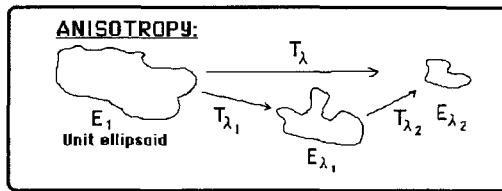
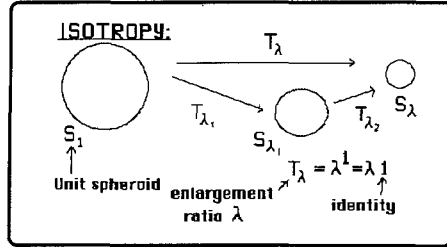


Figure 4a

Schematic illustration of the scaling (semi-) group $T_\lambda = \lambda^{-G}$ showing both isotropic (self-similar) and anisotropic cases. The basic properties are that if $\lambda = \lambda_1 \lambda_2$, then $T_\lambda = T_{\lambda_1} T_{\lambda_2}$. Furthermore, the “volume” of the ellipsoids is $\propto \lambda^{d_{el}}$ where $d_{el} = \text{Trace } G$.

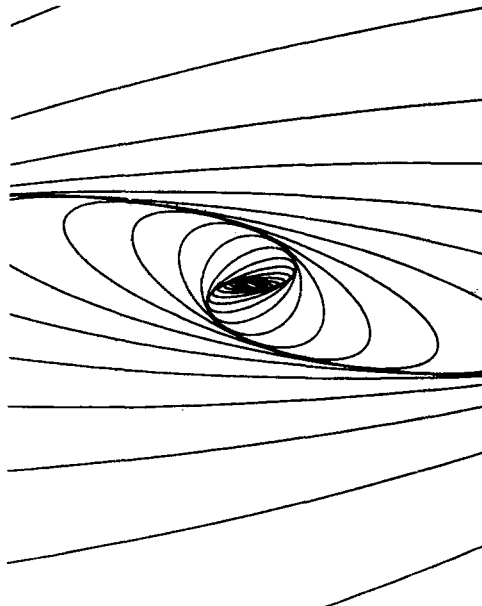


Figure 4b

Linear, self-affine balls with stratification dominant.

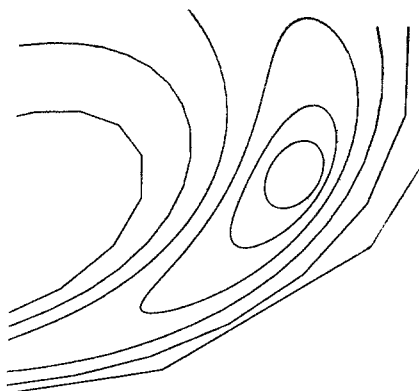


Figure 4c
Nonlinear examples of balls.

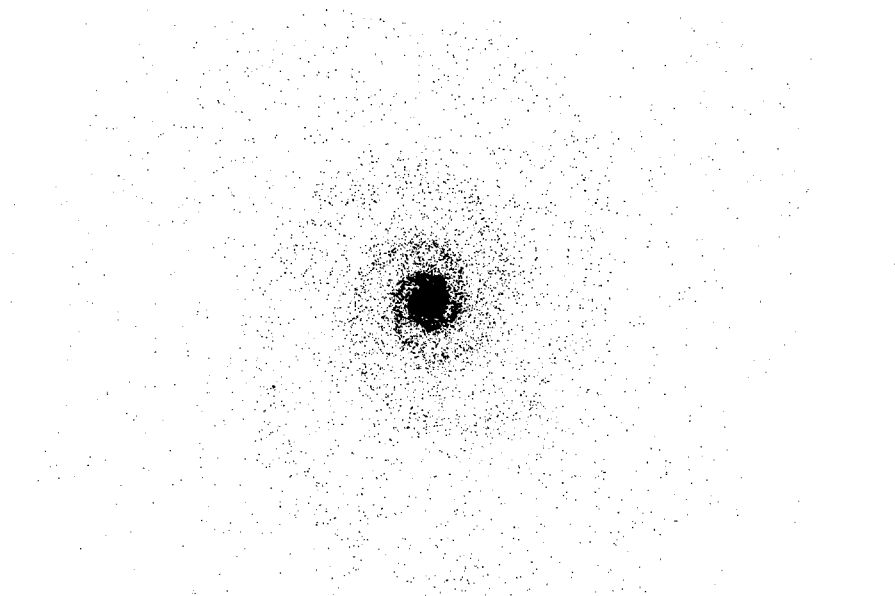


Figure 4d

A phenomenological galaxy model generated by 50,000 points (each representing a star) with positions $r = T_\lambda r'$ where r' is an isotropic vector in the plane with $\Pr(|r'| > R) \approx R^{-\alpha}$ with $\alpha = 0.10$ and $T_\lambda = \lambda^{-G}$ with $G = \begin{pmatrix} 1 & -6 \\ 8 & -6 \end{pmatrix}$ (linear GSI). Here, G was chosen so that rotation dominates yielding a (logarithmic) spiral galaxy. (For the decomposition of G into elementary basic matrices, see SCHERTZER and LOVEJOY, 1985a.)

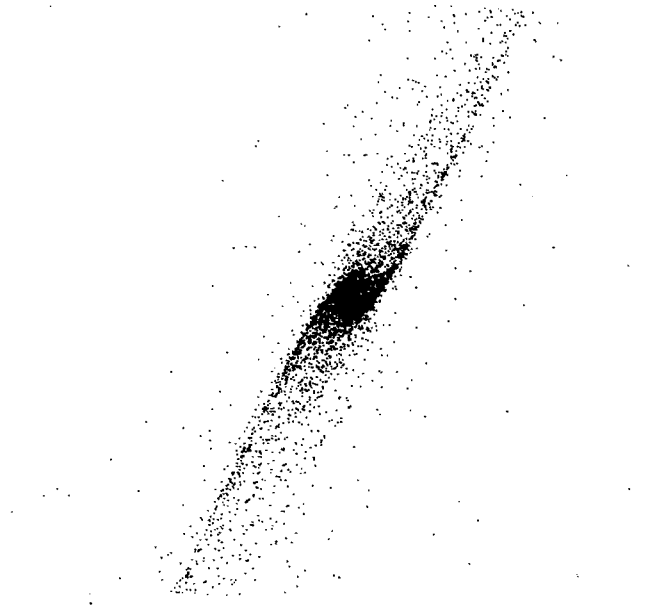


Figure 4e

Same as in Figure 4d except for 20,000 points, $\alpha = 0.25$, $\mathbf{G} = \begin{pmatrix} 1 & -0.08 \\ 2.08 & 0.25 \end{pmatrix}$, (implying that stratification dominates), yielding a “bar” galaxy.

certain ranges, that these fields are likely to be symmetric with respect to scale changing operations. This view is all the more compelling when it is realised that the requisite scale changes T_λ can be far more general than simple magnifications or reductions. In fact, it turns out that practically the only restriction on T_λ is that it had group properties, viz: $T_\lambda = \lambda^{\mathbf{G}}$ where \mathbf{G} is a the generator of the group of scale changing operations. In this “Generalised Scale Invariance” (“GSI”, see Figures 4a and section 5 below), \mathbf{G} can be either a matrix (“linear GSI”, self-similarity means $\mathbf{G} = \text{identity}$), or a more general nonlinear function (see Figures 4b,c). Figures 4d,e show how knowledge of this symmetry principle can produce simple models of galaxy structure (see section 5). In fact, it turns out that scale invariance allows for such a tremendous variety of behaviour (i.e., it is only a very weak constraint on the dynamics), that very little can be said *a priori* about scaling systems. Detailed data analysis and fractal models will doubtless be required to gain more insight into the relevant dynamics.

4. The Need for a General Formalism for Anisotropic Scale Invariance, the Example of the Atmosphere

A self-similar model of atmospheric turbulence could not hope to cover more than a very limited range of scales. This is obvious when one considers extrapolating using self-similarity, a roughly cubic cloud 1 km in size to a cloud a thousand

kilometers long—it would also be a thousand kilometers high, a possibility precluded by the strong atmospheric stratification. The classical schema of atmospheric motions (e.g., MONIN, 1972), attempts to overcome this difficulty by considering that atmospheric turbulence is three-dimensional at small scales but (a very different) two-dimensional turbulence at large enough scales. Due to numerous advances in remote and *in situ* measurements (see e.g., LILLY, 1983 or SCHERTZER and LOVEJOY, 1985b for reviews), it is now clear that single scaling regimes exist over most of the range of meteorologically significant scales in both the horizontal and vertical directions, although with very different scaling exponents (e.g., the horizontal wind has spectral exponents $\beta_h \approx 5/3$, $\beta_v \approx 11/5$ in the horizontal and vertical directions, respectively).

To avoid this untenable 2D/3D dichotomy, we have proposed an alternative scaling model of atmospheric dynamics (SCHERTZER and LOVEJOY, 1983a,b, 1984, 1985a,b,c 1986; see also LOVEJOY and SCHERTZER, 1986 for a nonmathematical review). In this model, the anisotropy introduced by gravity via the buoyancy force results in a differential stratification and a consequent modification of the effective dimension of space, involving a new elliptical dimension (d_{el}), with resulting anisotropic shears. In isotropy, $d_{el} = 3$, while in completely flat (stratified) flows, $d_{el} = 2$. Empirical and theoretical evidence were given indicating d_{el} is rather the intermediate value $d_{el} = 2 + (\beta_h - 1/(\beta_v - 1)) \approx 23/9 = 2.5555$.

In order to take into account this and other effects such as the differential rotation introduced by the Coriolis force, a general formalism of scaling is required. The fundamental problem is that of finding a family of “balls” representing the statistical properties of the eddies at different scales via (mathematical) random measures, such as the flux of energy through structures of a given scale. The first step is to generalise the notion of Hausdorff measures and the related (Hausdorff, fractal) dimensions in an anisotropic framework. We recall that such measures are rather straightforward extensions to noninteger D of the Lebesgue measure (defined for integer d), thus we use the notation $\int_A d^D x$ for the D -dimensional Hausdorff measure of a (compact) set A . The Hausdorff dimension $D(A)$ of A is still defined

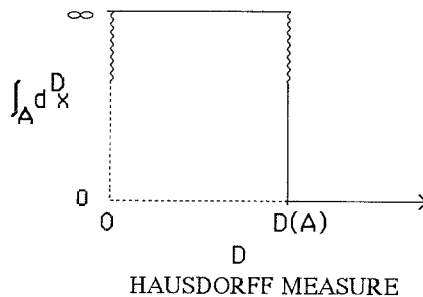


Figure 5
Divergence rule for Hausdorff measures.

by a divergence rule (“the length of a surface is infinite, the volume of it zero . . .”, see Figure 5):

$$\int_A d^D x = \infty, \quad \text{for } D < D(A); \quad \int_A d^D x = 0 \quad \text{for } D > D(A). \quad (5)$$

It turns out that the divergence of statistical moments are derived from a slightly more complex (twin) divergence rule (see section 6).

5. Generalised Scale Invariance (GSI)

Close examination of the phenomenology of turbulent cascades reveals the basic properties associated with the notion of scale: the (intermittent) concentration of the flux on sparser and sparser regions as the scale of homogeneity goes to zero. Thus scale changing is related to measurable properties of the flow, i.e., how the measure of the energy-flux becomes more and more intermittent (less and less homogeneous). We are lead to the following abstract definition in terms of a (semi-) group (the “scaling group”) of operators T_λ which reduce the scale by ratio λ (see Figure 3 for a schematic illustration)

$$T_\lambda = \lambda^{-G} = \exp(-G \log \lambda). \quad (6)$$

If G is not the identity, T_λ is no longer a mere contraction; and the eddies are no longer self-similar (when G is linear, and has no off-diagonal elements, the T_λ is self-affine). The consequence of this kind of transformation is that the energy flux is no longer evenly distributed on subsets with equal topological, and (isotropic) Hausdorff dimensions. For example, as soon as we anisotropically distribute the activity of turbulence (such as in Figure 2b), a vertical line is no longer equivalent to a horizontal one, etc.

In isotropy, scaling is based on three essential ingredients:

- A unit sphere
- The identity $\mathbf{1}$ as the generator of the self-similar scale changing transformation, ratio λ , ($T_\lambda = \lambda^{-1}$)
- The resulting scale notion ϕ (which is simply the radius of the sphere $S_\lambda = \lambda^{-1} S_1$, and at the same time, $\phi(S_\lambda) = \lambda^{-1} \phi(S_1) = \lambda^{-1}$).

Anisotropic scaling is based on the same ingredients, but with $T_\lambda = \lambda^{-G}$ with $G \neq \mathbf{1}$, and $\phi_{el}(T_\lambda S_1) = \lambda^{-1} \phi_{el}(S_1)$. The subscript “*el*” is used in the following to refer to the fact that in anisotropy, the scale-defining spheres are typically flattened ellipsoids (see Figure 4b). In fact much more general shapes are possible as soon as we use nonlinear generators: the balls need not even be convex (Figure 4c). Figures 4d,e give an example of linear GSI used as a phenomenological model for the structure of galaxies. The physical justification of such models rests on the fact that the electromagnetic and gravitational forces presumably responsible for galactic

structure, are scaling (power law), hence the resulting structure ought to respect the same scale invariant symmetries. Note that the natural classification of linear GSI into rotation or stratification dominant (SCHERTZER and LOVEJOY, 1985a) corresponds (at least visually) to spiral and “bar” galaxies, respectively.

The method of getting from the isotropic triple $\{S_1, \mathbf{1}, \phi\}$ with $\phi = (\int_A d^d x)^{1/d}$ to the anisotropic $\{S_1, \mathbf{G}, \phi_{el}\}$ is to test whether the generator \mathbf{G} has the required properties for the self-affine ellipsoids $E_\lambda = T_\lambda(S_1)$ rather than the self-similar spheres. In particular, are the E_λ decreasing with λ , and how can one define ϕ_{el} ? The answers to both these questions turn out to be simple (see SCHERTZER and LOVEJOY, 1985a), on condition that every (generalised) eigenvalue of \mathbf{G} has a nonnegative real part, i.e.

$$\inf \operatorname{Re} \sigma(\mathbf{G}) \geq 0$$

$$\sigma(\mathbf{G}) = \{\mu \in C \mid \mathbf{G} - \mu \mathbf{1} \text{ noninvertible on } CX\mathfrak{R}^d\} \tag{7}$$

$\sigma(\mathbf{G})$ being the (generalised) spectrum of \mathbf{G} , and ϕ_{el} is simply defined as

$$\phi_{el}^{d_{el}}(E_\lambda) = \phi^d(E_\lambda) = \lambda^{-d_{el}} \phi^d(S_1) = \lambda^{-d_{el}} \phi_{el}^{d_{el}}(S_1) \tag{8}$$

with $d_{el} = \operatorname{Tr}(\mathbf{G})$. Anisotropic Hausdorff measures of dimension D_{el} are simply defined as

$$\int_A d^{D_{el}} x = \lim_{\delta \rightarrow 0} \inf_{\substack{\cup E_i \supseteq A \\ \phi_{el}(E_i) < \delta}} \sum_i \phi_{el}^{D_{el}}(E_i) \tag{9}$$

since (due to eq. 8) $\phi_{el}^{D_{el}}(T_\lambda S_1) = \phi^D(T_\lambda S_1)$, with $D = (d/d_{el})D_{el}$, $\int_A d^{D_{el}} x$ is similar to $\int_A d^D x$ notwithstanding the difference that the former case, involves a covering by ellipsoids (E_i) rather than spheres (S_i) as in the latter. Nevertheless, if A is not “strange” (pathological), a near optimum covering (i.e., nearly equal to the infimum above) of ellipsoids can be associated with a near optimum covering of spheres (each of the ellipsoids is itself covered nearly optimally by smaller spheres). We can therefore expect the divergence rule for $\int_A d^{D_{el}} x$ and $\int_A d^D x$ to be the same. We have thus the following rule

$$D_{el}(A)/d_{el} = D(A)/d. \tag{10}$$

Nevertheless, it is important to point out exceptions of particular importance: if A is restricted to a (generalised) eigenspace E_i of \mathbf{G} , then the preceding rule must be rewritten:

$$D_{eli}(A)/d_{eli} = D(A)/d_i \tag{11}$$

where d_i is the topological dimension of E_i , d_{eli} its anisotropic dimension i.e., $d_{eli} = \operatorname{Tr}(G|_{E_i})$; $G|_{E_i}$ being the restriction of \mathbf{G} on E_i .

Using anisotropic scale changing operators rather than isotropic ones, it is straightforward to transform self-similar stochastic processes into their anisotropic counterparts. Figure 6 gives an example of vertical cloud cross-section obtained by

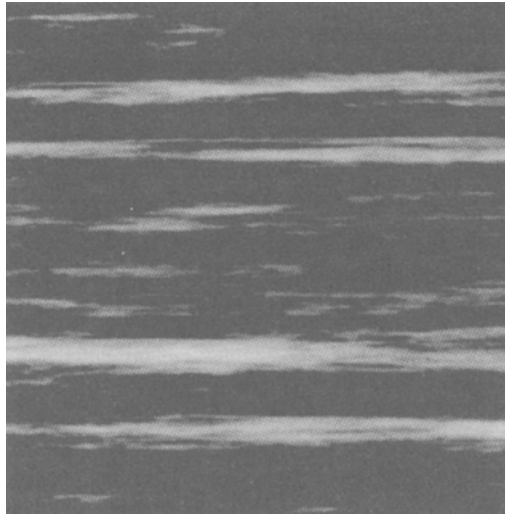


Figure 6
A cross-section of an anisotropic, fractal sums of pulses process with $d_{et} = 2.555$.

modifying the fractal sums of pulses process (LOVEJOY and MANDELBROT, 1985) so as to simulate a cross-section of a 2.555 dimensional cloud (see LOVEJOY and SCHERTZER, 1985). More elaborate processes (such as those discussed below) can be rendered anisotropic by using similar techniques.

6. GSI and Multiple Singularities

Instead of adding random increments of finer and finer resolution along the cascade (as in Figure 6), one may multiply by random increments of finer and finer resolution. This multiplicative procedure corresponds to the nonlinear break-up of eddies into sub-eddies, and is the natural process to study in turbulence, since the scale changing operator that transforms large eddies into small eddies, itself forms a multiplicative group.

Unlike additive processes where the limit as the cascade scale approaches zero is a function, the corresponding limit of multiplicative processes (also called “multiplicative chaos”) is very singular. This limit is no longer a function, but an operator converting one measure into another (e.g., the $D(A)$ - “volume” of A into the energy flux through A). The situation can be imagined as follows: as we introduce finer and finer scale ($l_n = l_0/\lambda^n$) multiplicative perturbations, the density (ε_n) of the energy flux becomes increasingly dominated by singularities (positive γ_n):

$$\Pr (\varepsilon_n \geq \varepsilon_0 \lambda^{\gamma_n}) \approx \lambda^{-c_n(\gamma_n)} \tag{12}$$

(see examples, Figures 3,7) where “Pr” means “probability”. In the limit $n \rightarrow \infty$

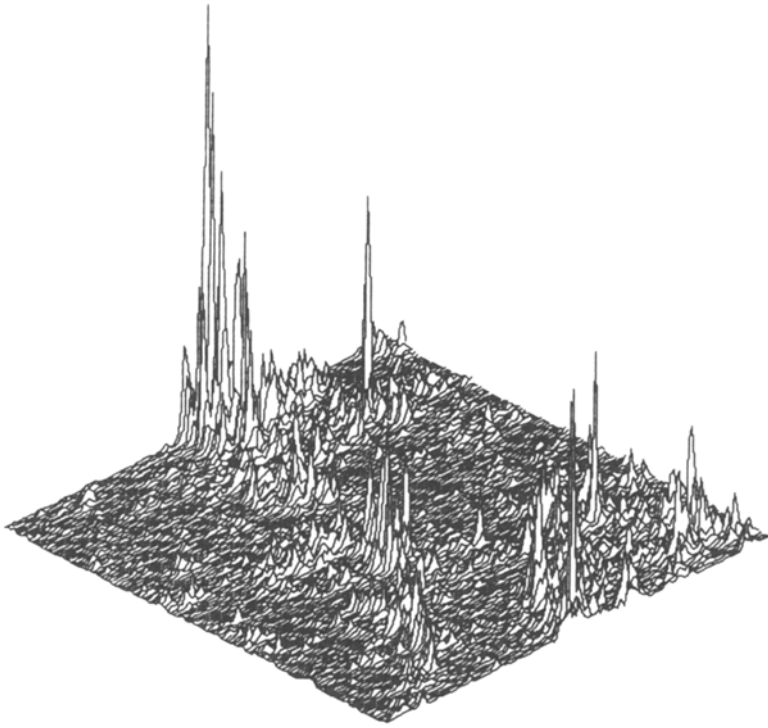


Figure 7
 Multiplicative process on a 128×128 square grid.

(writing $\gamma_n \rightarrow \gamma$ and $c_n \rightarrow c$) we can interpret this equation as indicating that those singularities of order higher than a given level γ , being distributed over a fractal set of codimension $c(\gamma)$, which becomes sparser with increasing γ since $c(\gamma)$ is an increasing function. These singularities prevent convergence in the usual sense. However, by “integrating” the result over a set A with dimension $D(A)$ (to obtain the flux through A), the resulting smoothing may be sufficient so that convergence is obtained at least for low order statistics. Convergence of statistical moments of order h ($h > 1$) is assured by the convergence of the “ h^{th} trace moment” (SCHERTZER and LOVEJOY, 1987a,b) may be defined as:

$$\begin{aligned} \langle \text{Tr}_{A_n} \varepsilon_n^h \rangle &= \int_{A_n} \varepsilon_n^h d^{hD}(A)x \\ \langle \text{Tr}_A \varepsilon^h \rangle &= \lim_{n \rightarrow \infty} \langle \text{Tr}_{A_n} \varepsilon_n^h \rangle \end{aligned} \tag{13}$$

where A_n is A with a resolution l_n (i.e., we compute the Hausdorff measure (Eq. 5) by covering only with balls of size greater than that of the inhomogeneity). Since the latter quantity is of the same type as a Hausdorff measure (SCHERTZER and LOVEJOY, 1987a,b), it is not surprising that it follows a twin divergence rule

(represented in Figure 8), implying the convergence of statistics of order h , for $C(h) < D(A)$ ($h > 1$) and divergence otherwise, where $C(h)$ is the codimension function defined by the trace moments. Conversely, for $h < 1$, we obtain $C(h) > D(A)$ implying degeneracy of the flux (it is almost surely zero).

Since a multiplicative group (parameter λ , the generalised ratio of scales) is involved, the characterisation of its intermittency generator γ is fundamental. It results that it should be “1/f noise” (its spectrum being proportional to the inverse of the wave-number) in order to assure a logarithmic divergence of its “free energy” (or its second characteristic functional) which is required to obtain scaling of the resulting field. The codimension functions $c(\gamma)$, $C(h)$ are thus related to each other by a Laplace transformation (which may reduce to a Legendre transformation in certain, but not all cases). Figure 7 results from a simulation using a gaussian “1/f noise”, but Levy noise could also be used. Using this type of continuous cascade construction of a “multifractal measure”, it was further shown (SCHERTZER and LOVEJOY, 1987a,b; 1988b) that continuous cascade processes define universality classes in which $c(\gamma)$ is of the form

$$c(\gamma) = c_0(1 + \gamma/\gamma_0)^\alpha \tag{14}$$

where $\alpha \geq 2$, with the value $\alpha = 2$ corresponding to the case of gaussian cascade generator, and c_0, γ_0 are parameters characterising respectively the intermittency and smoothness of the process.

The codimension functions $c(\gamma)$ and $C(h)$ (determining the fraction of the (sub-)space where singularities or divergences occur) are directly connected to the generator γ of intermittency. Hence, when the latter is expressed in a given framework, defined by the anisotropic generator G with corresponding d_{el} (i.e., γ and G commute), these two functions remain the same for any restriction of the process on a (generalised) eigenspace of G (this is analogous to the isotropic case). This remark is of particular importance for data analysis of anisotropic fields: one seeks to determine the anisotropy generator yielding such an invariance of the

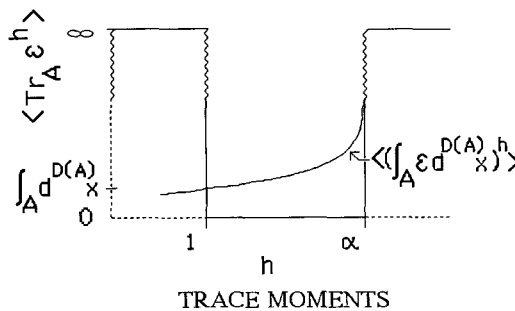


Figure 8
Twin divergence rule of the trace moments.

codimension functions or at least the corresponding elliptical dimension. For other relevant references to singularities and multiplicative processes, see KAHANE (1985), PIETRONERO and SIEBESMA (1986), HALSEY *et al.* (1986) and LEVICH and SHTILMAN (1988) as well as the minireview by STANLEY and MEAKIN (1988).

7. Elliptical Dimensional Sampling and the Empirical Evaluation of d_{el} in Rain

7.1 The Data

In this section we estimate d_{el} and $c(\gamma)$ for radar rain reflectivities. These reflectivities are probably the geophysical data of highest quality available for this purpose. The rain drops act as efficient natural tracers, allowing the 3-D rain structure to be quickly and nonperturbatively sampled. At the McGill weather radar observatory, archives contain data spanning over two orders of magnitude in each horizontal direction, one in the vertical, five in time, and six in intensity (reflectivity, denoted Z). The actual data analysed here were resampled in (r, θ, z) (range, azimuth and height above the earth's surface), from the original polar (r, θ, ϕ) coordinates, with $(200 \times 375 \times 8)$ resolution elements, with intensities in 16 logarithmic levels, 4 dBZ apart (factor ≈ 2.5). The whole scale therefore spans a range of $15 \times 4 = 60$ dBZ = factor of 10^6 . It is not uncommon for reflectivity levels in rain to exceed 10^5 times the minimum detectable signal.

Physically, the reflectivity is simply the integrated backscatter of the rain drops. The microwave reflectivity for each drop (here at 10 cm wavelength) is proportional to V^2 (where V is the rain drop volume). At 10 cm, the absorption is sufficiently small that the beam is nearly unattenuated. The reflectivity Z measured in this way is the integral over an entire "pulse" volume (roughly 1 km^3) of V^2 of each drop modulated by its phase. Operational (meteorological) use of radar data is limited primarily by the fact that the rain rate (R) is a different integral: that the product of V and the fall speed. The standard semi-empirical (and very rough) relationship between R and Z is called the Marshall-Palmer formula: $Z = 200 R^{1.6}$ with Z in $(\text{mm})^6 \text{m}^{-3}$, and R in mm/hr. It is important to note that by directly studying relative reflectivities rather than R , we avoid the traditional radar calibration problem. Noise and instrumental biases are small.

7.2 Functional Box-Counting

Since we expect multiple dimensions (or dimension functions, rather than single values), we have to generalise the usual "box-counting" algorithm (designed to estimate the dimension of a set of points, e.g., HENTSCHEL and PROCCACIA (1983)) so as to apply it to fields ("functional box-counting", LOVEJOY *et al.*, 1987). This is achieved (as shown in Figure 9) by thresholding the fields (with various threshold

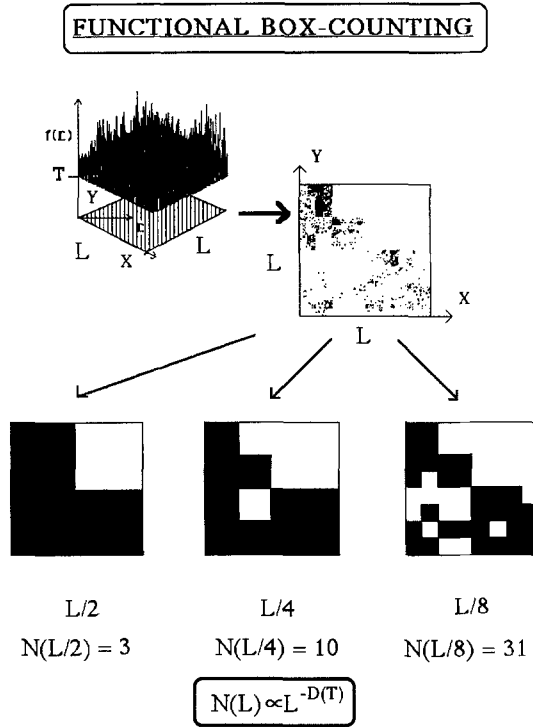


Figure 9

Schematic illustration of functional box-counting. In the first step (upper left), the initial field $f(\underline{r})$ is threshold to yield the exceedance set (upper right). On the line below, reduced versions of this figure are covered with boxes of decreasing scale (size, left to right, one half, one quarter and one eighth of the scale of the original).

T_i) and determining the corresponding hierarchy of dimensions $D(T_i)$ (approximating them by $N(L) \approx L^{-D(T_i)}$, $N(L)$ being the number of boxes, of size L , needed to cover the set (defined by those regions exceeding the threshold).

When $N_T(L) \approx L^{-D(T)}$ with $D(T) < d$, the fraction of the image exceeding T decreases with increasing resolution as $L^d L^{-D(T)} = L^{C(T)} \rightarrow 0$ as $L \rightarrow 0$. This is the counterpart of eq. (12) which shows that the field values corresponding to a given dimension diverge at a rate depending on the order of their associated singularity. In order to estimate the scale invariant (resolution independent) function $c(\gamma)$ and hence to test the prediction that it has universal form (eq. 14), for each field value, at scale L (denoted T_L) we associate a singularity of order γ as follows

$$T_L/T_0 = (L/L_0)^{-\gamma} . \tag{15}$$

T_0 is the field value at a reference scale. Now, taking T_L as the intrinsic resolution of the detector and T_0 as the mean field over the entire image, we obtain

$$\gamma = -\log(T_L/T_0)/\log(L/L_0) \tag{16}$$

where L/L_0 is the ratio of scales between the intrinsic resolution and the scale of the entire image. Eliminating T , in terms of γ using (eq. 16), we thus obtain the entirely resolution independent function $c(\gamma)$.

When such a functional box-counting is applied to the radar reflectivity data for a single radar scan, we obtain the results shown in Figures 10a,b. In the horizontal, we have used sectorial (pie-shaped) boxes, increasing the angular and downrange

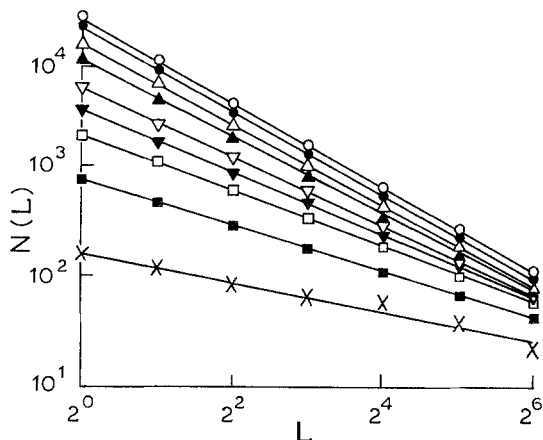


Figure 10a

$N(L)$ vs L for the nine radar reflectivity thresholds described in the text, for a single radar volume scan, analysed with horizontal boxes increasing by factors of two in linear scale (data corresponding to a Montreal summer, convective shower). All correlation coefficients of $\log N$ vs $\log L$ were > 0.99 . For clarity, only every second threshold symbol is shown at left, with values representing the ratio of the reflectivities to the minimum detectable signal. The negative slope, D , decreases from 1.24 to 0.40.

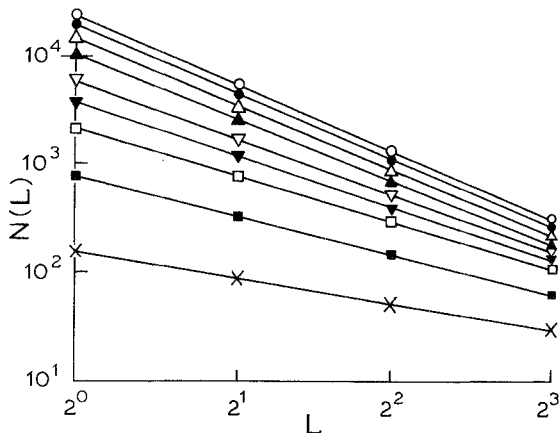


Figure 10b

Same as Figure 10a, except that the boxes used are cubical (three-dimensional, rather than squares). Here D decreases from 2.18 to 0.81. Only 8 different vertical levels were available.

box sizes by factors of 2, starting with the highest resolution available (the use of pie-shaped boxes eliminates all range-dependent effects due to beam spreading, etc.). The straightness of the lines shows that scaling is accurately followed in both horizontal and vertical directions. Note the systematic decrease in the absolute slope ($=D(\gamma)$) as γ is increased (here through 9 values with corresponding thresholds separated by 4 dBZ spanning a total range of reflectivity of $10^{(9-1)0.4} \approx 40,000$ — γ varies from 0 to ≈ 2). Of twenty radar volume scans studied, all the horizontal $D(\gamma)$ values calculated by regressions of $\log N(\gamma)$ vs $\log \gamma$ resulted in correlation coefficients > 0.99 , when γ was in the range (for the lowest 6 thresholds, where $N(L)$ was fairly large, the correlation coefficient was > 0.999). For even higher values of γ , $N(L)$ was too small to give reliable estimates of $D(\gamma)$.

Recently, (GABRIEL *et al.*, 1986, 1988) have applied this technique to visible and infra-red satellite pictures of both clouds and surface features in the range 8 to 512 km. Their results clearly show the scaling of both fields and have important consequences for satellite remote sensing, since scaling generally implies strong (and undesirable) resolution dependencies in quantities (such as fractional cloud cover) estimated from the satellite. The finding of multiple scaling in visible albedoes and IR emission from (cloud-free) land surfaces confirms that scaling is likely to a property of many geophysical surface features.

7.3 Elliptical Dimensional Sampling

We can now apply functional box-counting to horizontal cross-sections and volumes (Figures 10a,b), determining the functions $D_2(\gamma)$ and $D_3(\gamma)$ respectively, and use the difference between the two to obtain a characterisation of the degree of horizontal stratification in rain. If the rain field was isotropic, then $D_2(\gamma)$, $D_3(\gamma)$ can be simply related to each other by the identity of their corresponding codimensions:

$$\begin{aligned} C_3(\gamma) &= C_2(\gamma) \\ C_d(\gamma) &= d - D_d(\gamma) \end{aligned} \quad (17)$$

We have already noted the generalisation of these relations in anisotropy, so that the correct elliptical dimension d_{el} of the rain field should satisfy

$$\begin{aligned} C_{d_{el}}(\gamma) &= C_2(\gamma) \\ C_{d_{el}}(\gamma) &= d_{el} - D_{d_{el}}(\gamma) \end{aligned} \quad (18)$$

We thus sample (see illustration in Figure 11) the data using a family of self-affine boxes—with corresponding generators G 's and associate elliptical dimensions D_{el} 's—seeking the zero of the following function

$$f(D_{el}) = \sum_i^k (C_{D_{el}}(\gamma_i) - C_2(\gamma_i)) \quad (19)$$

with the empirical C 's determined by the functional box-counting, and the sum is

ELLIPTICAL BOX COUNTING

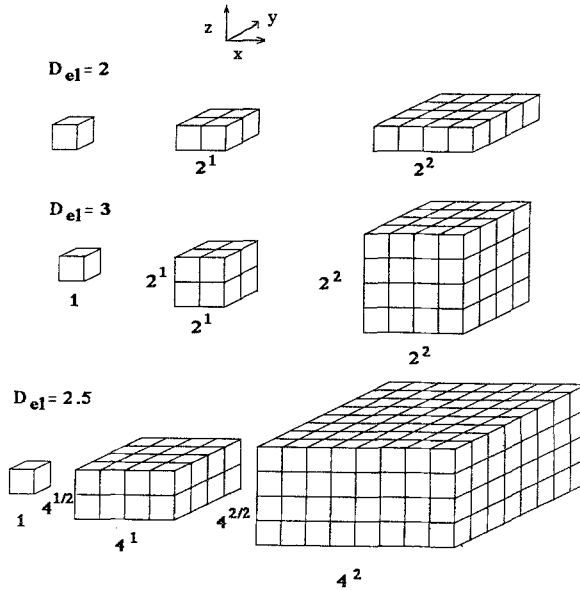


Figure 11

Elliptical dimensional sampling. Showing the shapes of the “elliptical” boxes used in box counting at increasing scales with $d_{el} = 2, 3, 2.5$.

over the k thresholds (=9 here). Furthermore, due to the linearity of eq. (10), $f(D_{el})$ is linear in D_{el} .

Figure 12 shows the result as D_{el} is varied through 15 values between 3 and 2.13, which was roughly the lowest value accessible with the data set (corresponding to boxes of $1 \times 1 \times 1$ pixel and boxes $190 \times 190 \times 2$ pixels, twice the anisotropic scale, where $2.13 = 2 + \log 2 / \log 190$). The same nine thresholds were used as before.

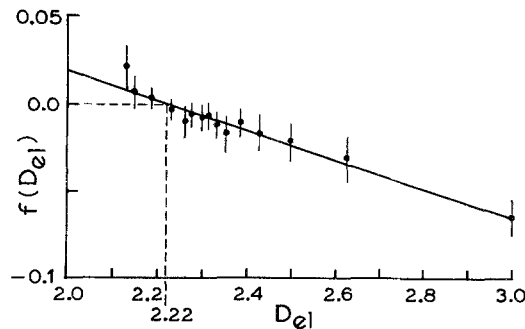


Figure 12

The function $f(D_{el})$ described in the text which is the average of data taken from 20 scans, using 15 different values of D_{el} , and 9 reflectivity thresholds (= $9 \times 15 \times 20 = 2700$ dimensions). The least squares linear regression (correlation coefficient = 0.98), is shown, cutting the axis at $D_{el} = d_{el} = 2.22$.

$f(D_{el})$ was determined separately on 20 radar rain fields: Figure 12 shows the averages and standard deviations (indicated by the error bars). The linear regression shown, yields $d_{el} = 2.22 \pm 0.07$. The error is the standard deviation of d_{el} estimated from each of the 20 images separately (see LOVEJOY *et al.*, 1987 for more details). It is interesting to note that this value is considerably smaller than the value $d_{el} = 23/9 = 2.555$ found for the horizontal wind field.

7.4 The Universality of $c(\gamma)$

We now show that the empirical $c(\gamma)$ functions fit into the universality classes (eq. 14). For the radar data used here (the same data set discussed in 7.1), the empirically accessible range of γ 's is quite small (the maximum is ≈ 2.0). This makes it difficult to accurately estimate α since the latter measures the concavity of $c(\gamma)$ which is only pronounced for large γ . The difficulty is that if eq. (14) is considered to define a multiparameter regression problem for the coefficients c_0, γ_0, α , as determined from the various empirical values $c(\gamma)$, then all three parameters are highly correlated with each other and the optimum values are ill-defined. To obtain well-defined estimates, we therefore made the plausible assumption that generators were in the gaussian domain of attraction (i.e., $\alpha = 2$), and for each radar image, we empirically estimated the parameter γ_0 via a least squares regression using the formula

$$c_n(\gamma) = c(\gamma)/c(0) = (1 + \gamma/\gamma_0)^2 \tag{20}$$

where $c_n(\gamma)$ is the codimension "normalised" by $c(0)$ which is the empirically determined codimension of the field at average brightness (since $T = T_0 \Rightarrow \gamma = 0$).

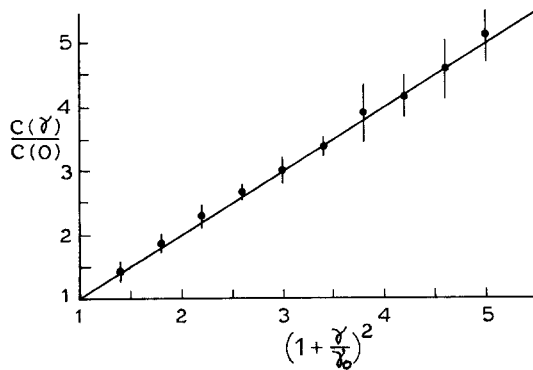


Figure 13

The mean normalised codimension, $\langle c_n(\gamma) \rangle$ for the radar data, analysed in Figure 10 (with one standard deviation error bars) plotted against the mean $\langle (1 + \gamma/\gamma_0)^2 \rangle$ to test whether the empirical $c(\gamma)$ functions belong to the universality class defined by $\alpha = 2$ ($c(0)$ is measured directly, and γ_0 is determined by regression for each image separately). A perfect fit (corresponding to the line $x = y$) is shown for reference.

The standard error of the fit (of $c(\gamma)$) in all 20 cases, over the entire range of $c(\gamma)$, was ± 0.062 which is comparable to the errors in determining $c(\gamma)$ from the box-counting algorithm. We then plot the curves $\langle c_n(\gamma) \rangle$ vs $\langle (1 + \gamma/\gamma_0)^2 \rangle$ in Figure 13 where the angle brackets indicate ensemble averaging (here all available cases). As predicted by eq. (20), the curves all closely follow the line $x = y$ (shown for reference). This shows that the main difference between the various radar images cases were in the values of the parameters. Similar results (also for $\alpha = 2$) for visible and IR satellite images can be found in GABRIEL *et al.* (1988a).

8. Conclusions

We have argued that highly intermittent anisotropic atmospheric fields can be best understood and quantitatively studied in the framework of Generalised Scale Invariance (GSI). This formalism is a development of phenomenological models of anisotropic turbulent cascades, but applies generally to anisotropic scale invariant geophysical fields. Within GSI, singularities of the fields of interest are generated (or analysed in terms of) two multiplicative one-parameter semi-groups. The first defines the anisotropy from scale to scale, and the second, the concentration of the field into sparser and sparser regions, for higher and higher order singularities. The resulting stratification and intermittency have no characteristic scale.

These groups define two (dual) "elliptical" codimension functions $C(h)$ and $c(\gamma)$. The former prescribes the divergence of the h^{th} order statistical moments of the flux over regions A of dimension $D(A) < C(h)$ ($h > 1$) or its degeneracy ($h < 1$), while the latter describes the distribution of the (multiple) singularities exponents γ . The admissible generators of these semi-groups are a) all those operators \mathbf{G} having eigenvalues with nonnegative real parts and b) all intermittency generators γ with logarithmic divergence of the free energy (second characteristic functional) with the scale of homogeneity. Whereas standard statistical mechanics involves stationary (conserved) energy, these multiplicative processes involve stationary energy fluxes. We have shown that flux dynamics differs radically from normal dynamics because of the singular nature of the small scale limiting properties. In particular, in flux dynamics, observables are expected to have extremely intermittent behaviour characterised by the divergence of high order statistical moments.

To illustrate these ideas, we described how multiplicative processes can be modelled numerically. We discussed anisotropic scale invariant models of clouds and galaxies.

Empirically, we showed evidence obtained from blotting paper analyses of raindrop distributions showing that scaling holds at very small scales. At scales of kilometers, we used radar reflectivities to obtain a direct estimate of the elliptical dimension characterising the degree of stratification the rain field: $d_{el} = 2.22 \pm 0.07$. In the latter case, we also determine empirical codimension functions that were described by two-parameter universality classes.

Acknowledgements

We acknowledge discussions with, G. L. Austin, P. Gabriel, P. Ladoy, D. Lavallée, E. Levich, J. P. Muller, A. Saucier, A. A. Tsonis, R. Viswanathan, T. Warn, and J. Wilson.

REFERENCES

- FRISCH, U., P. L. SULEM, and M. NELKIN (1978), *A simple dynamical model of intermittency in fully developed turbulence*. J. Fluid Mech. 87, 719–724.
- FRISCH, U. and G. PARISI, *A multifractal model of intermittency*. In *Turbulence and Predictability in Geophysical Fluid Dynamics and Climate Dynamics* (eds. Ghil, Benzi, Parisi) (North-Holland, 1985), pp. 84–88.
- GABRIEL, P., S. LOVEJOY, G. L. AUSTIN and D. SCHERTZER (1986), *Radiative transfer in extremely variable fractal clouds*, 6th Conference on Atmospheric Radiation 230–236, AMS, Boston.
- GABRIEL, P., S. LOVEJOY, and D. SCHERTZER (1988a), *Multifractal analysis of resolution dependence in satellite imagery*. Geophys. Res. Letter (in press).
- GABRIEL, P., S. LOVEJOY, and D. SCHERTZER (1988b), *Discrete angle radiative transfer in fractal clouds*. In *Scaling, Fractals and Non-Linear Variability in Geophysics* (eds. D. Schertzer, S. Lovejoy) (Kluwer), in press.
- HALSEY, T. C., M. H. JENSEN, L. P. KADANOFF, I. PROCACCIA, and B. I. SHRAIMAN (1986), *Fractal measures and their singularities: the characterisation of strange sets*. Phys. Rev. A 33, 1141–1151.
- HENTSCHEL, H. G. E. and I. PROCACCIA (1983), *The infinite number of generalised dimensions of fractals and strange attractors*, Physica 8D, 435–444.
- HUBERT P. and J. P. CARBONNEL (1988), *Caractérisation Fractale de la variabilité et de l'anisotropie des précipitations intertropicales*. C.R. Acad. Sci. Paris 2, 307, pp. 909–914.
- KAHANE, J. P. (1985), *Multiplicative chaos*. Ann. Math. du Quebec 9, 435–444.
- KEDDEM, B. and L. S. CHIU (1987), *Are rain rate processes self-similar?* Wat. Resour. Res. 23, 1816–1818.
- KOLMOGOROV, A. N. (1962), *A refinement on local structure of turbulence*. Mécanique de la Turbulence 447, Editions du CNRS, France.
- LAVALLÉE D., D. SCHERTZER, and S. LOVEJOY (1988), *On the determination of the codimension function*. In *Scaling, Fractals and Non-Linear Variability in Geophysics* (eds. D. Schertzer, S. Lovejoy) (Kluwer), in press.
- LEVICH, E. and I. SHTILMAN (1988), *Helicity fluctuations and coherence in developed turbulence*. In *Scaling, Fractals and Non-Linear Variability in Geophysics* (eds. D. Schertzer, S. Lovejoy) (Kluwer), in press.
- LILLY, D. K., *Mesoscale variability of the atmosphere*. In *Mesoscale Meteorology-Theories, Observations and Models* (eds. D. K. Lilly and T. Gal'Chen) (Reidel, New York, 1983), pp. 13–24.
- LOVEJOY, S. and B. MANDELBROT (1985), *Fractal properties of rain and a fractal model*. Tellus 37A, 209–232.
- LOVEJOY, S. and D. SCHERTZER (1985), *Generalised scale invariance and fractal models of rain*. Wat. Resour. Res. 21, 1233–1250.
- LOVEJOY, S. and D. SCHERTZER (1986), *Scale invariance, symmetries, fractals and stochastic simulations of atmospheric phenomena*. Bulletin of the AMS 67, 21–32.
- LOVEJOY, S., D. SCHERTZER, and P. LADOY (1986a), *Fractal characterisation of inhomogeneous geophysical measuring networks*. Nature 319, 43–44.
- LOVEJOY, S., D. SCHERTZER, and P. LADOY (1986b), *Brighter outlook for weather forecasting*. Nature 320, 411.
- LOVEJOY, S., D. SCHERTZER, and A. A. TSONIS (1987), *Functional box-counting and multiple elliptical dimensions in rain*. Science 235, 1036–1038.
- LOVEJOY, S. and D. SCHERTZER (1988a), *Meeting Report: Scaling, fractals and nonlinear variability in geophysics*. EOS 69, 143–145.

- LOVEJOY, S. and D. SCHERTZER (1988b), *Multifractal analysis techniques and the rain and cloud fields from 10^{-3} to 10^6 m.* In *Scaling, Fractals and Non-Linear Variability in Geophysics* (eds. D. Schertzer, S. Lovejoy) (Kluwer), in press.
- LOVEJOY, S. and D. SCHERTZER (1988c), *Comments on "Are rainrates self-similar?"* Wat. Resour. Res. (submitted 10/12/87).
- LOVEJOY, S. and D. SCHERTZER (1988d), *Extreme variability, scaling and fractals in remote sensing: Analysis and simulation.* In *Digital Image Processing in Remote Sensing* (ed. P. J. Muller) (Taylor and Francis, London), in press.
- MANDELBROT, B. (1974), *Intermittent turbulence in self-similar cascades: Divergence of high moments and dimension of the carrier.* J. Fluid Mech. 62, 331–350.
- MANDELBROT, B., *The Fractal Geometry of Nature* (Freeman, New York, 1982) pp. 465.
- MARQUET O. and J. M. PIRIOU (1987), *Thesis, Météorologie Nationale, Toulouse, France.*
- MONTARIOL, F. and R. GIRAUD (1986), *Thesis, Météorologie Nationale, Toulouse, France.*
- MONIN, A. S., *Weather Forecasting as a Problem in Physics* (MIT Press, Cambridge, MA, 1972).
- NOVIKOV, E. A. and R. STEWART (1964), *Intermittency of turbulence and spectrum of fluctuations in energy-dissipation.* Izv. Akad. Nauk. SSSR. Ser. Geofiz. 3, 408.
- OBUKHOV, A. M. (1962), *Fluctuations of the energy dissipation in turbulence.* J. Geophys. Res. 67, 3011–3014.
- PIETRONERO, L. and A. P. SIEBESMA (1986), *Self-similarity of fluctuations in random multiplicative processes.* Phys. Rev. Lett. 57, 1098–1101.
- SCHERTZER, D. and S. LOVEJOY (1983a), *The dimension of atmospheric motions*, Preprints, IUTAM Symp. on Turbulence and Chaotic Phenomena in Fluids, 141–144, Kyoto, Japan.
- SCHERTZER, D. and S. LOVEJOY (1983b), *On the dimension of atmospheric motions*, Proceedings, 4th Symp. of Turbulent Shear Flows, 11.1, 11.8.
- SCHERTZER, D. and S. LOVEJOY, *Turbulence and Chaotic Phenomena in Fluids* (ed. T. Tatsumi) (North-Holland 1984) pp. 505–508.
- SCHERTZER, D. and S. LOVEJOY (1985a), *Generalised scale invariance in turbulent phenomena.* P.C.H. Journal 6, 623–635.
- SCHERTZER, D. and S. LOVEJOY (1985b), *The dimension and intermittency of atmospheric dynamics.* Turbulent Shear Flow 4, 7–33, (ed. B. Launder) (Springer).
- SCHERTZER, D. and S. LOVEJOY (1985c), *Generalised scale invariance in rotating and stratified turbulent flows*, Proceedings 5th Conference on Turbulent Shear Flow, 13.1–13.6.
- SCHERTZER, D. and S. LOVEJOY, *Generalised scale invariance and anisotropic intermittent fractals.* In *Fractals in Physics*, (eds. Pietronero, Tosatti) (North-Holland 1986), pp. 457.
- SCHERTZER, D. and S. LOVEJOY (1987a), *Physical modelling of rain and clouds as anisotropic, scaling and turbulent cascade processes.* J. Geophys. Res. 92, 9693–9714.
- SCHERTZER, D. and S. LOVEJOY (1987b), *Annales Math. du Que.* 11, 139–181.
- SCHERTZER, D. and S. LOVEJOY (1988a), *Scaling, Fractals and Non-Linear Variability in Geophysics* (Kluwer), in press.
- SCHERTZER, D. and S. LOVEJOY (1988b), *University classes in multiplicative processes.* In *Scaling, Fractals and Non-Linear Variability in Geophysics* (eds. D. Schertzer and S. Lovejoy) (Kluwer), in press.
- STANLEY, H. E. P. and P. MEAKIN (1988), *Minireview on multifractals.* Nature (in press).
- YAGLOM, A. M. and A. S. MONIN, *Statistical Hydrodynamics* (MIT Press 1975).

(Received June 3, 1987, revised May 2, 1988, accepted June 5, 1988)